Hindawi
Advances in Civil Engineering
Volume 2018, Article ID 9179343, 14 pages
https://doi.org/10.1155/2018/9179343

Research Article

Biaxial Shear Load Capacity of Anchor System for Quick-Hardening Track on Railway Bridges

Kyoung Chan Lee,[1] **Il-Wha Lee**,[1] **and Seong-Cheol Lee**[2]

[1]*Advanced Railroad Civil Engineering Division, Korea Railroad Research Institute (KRRI), 176 Cheoldobangmulgwan-ro, Uiwang-si, Gyeonggi-do 16105, Republic of Korea*
[2]*Department of Civil Engineering, Kyungpook National University, 80 Daehakro, Bukgu, Daegu 41566, Republic of Korea*

Correspondence should be addressed to Seong-Cheol Lee; seonglee@knu.ac.kr

Received 2 April 2018; Accepted 22 July 2018; Published 4 September 2018

Academic Editor: Arnaud Perrot

Copyright © 2018 Kyoung Chan Lee et al. This is an open access article distributed under the Creative Commons Attribution License, which permits unrestricted use, distribution, and reproduction in any medium, provided the original work is properly cited.

Quick-hardening railway track was developed to rapidly convert old-style ballast track to slab track in order to improve its maintainability and ride comfort. On bridges, quick-hardening track is applied in a segmented structure to reduce the temperature constraint, and anchors at the centers of the segments securely couple the track to the bridge. In this study, an anchor system is proposed that facilitates fast construction, and two designs for the proposed anchor systems are provided along with experimental test results of the same. Two anchor system designs were developed to allow for the maximum possible longitudinal and transverse loads in high-speed railways while considering the frictional resistance between the track slab and bridge deck. The biaxial shear capacity of each design was investigated experimentally, and the structural capacity for biaxial shear loads was evaluated using an elliptical curve to represent the longitudinal and transverse shear capacities. The minimum friction coefficient was determined based on the results of the evaluation to minimize damage to the anchor. The results obtained from the experiments confirmed that the proposed anchor systems possess sufficient shear capacity for application on high-speed railway bridges.

1. Introduction

In ballast tracks, the operation of trains causes the movement, rearrangement, abrasion, and penetration of ballast particles, which results in continuous plastic deformation of the ballast layer and gradually leads to railway warping (i.e., track irregularity). To ensure safe train operation, it is imperative that the track geometry be maintained, which therefore requires the ballast layer to be continuously maintained. However, even with periodic maintenance, the lifetime of ballast tracks is expected to be no longer than about 30 years [1]. In the time since high-speed trains operating at 300 km/h were introduced, the incidence of ballast track irregularities has increased, which has increased the maintenance costs accordingly.

In contrast to a ballast track, a slab track does not exhibit track irregularities because it is highly stable and requires little maintenance. However, replacing an existing ballast track with a slab track is a time-intensive process requiring many working days during which the track cannot be used. Thus, to continue operating while the track is replaced, railways must build a bypass loop around the current railway line. To reduce the cost and complexity of installing a slab track, a quick-hardening track technique based on quick-hardening mortar has been developed that drastically shortens the track replacement period [2–5]. As illustrated in Figure 1, the quick-hardening track technique constructs a slab track by collecting and cleaning existing ballast gravel from old ballast tracks and then recasts and hardens them with quick-hardening mortar. As this technique requires only three or four hours to complete, it is suitable for nighttime application when no trains are running and, most importantly, it does not require the current railway line to be shut down during the replacement process. Recently, the behavior of quick-hardening track on an earthwork section was analyzed by considering the thermal stress [2], quick-hardening

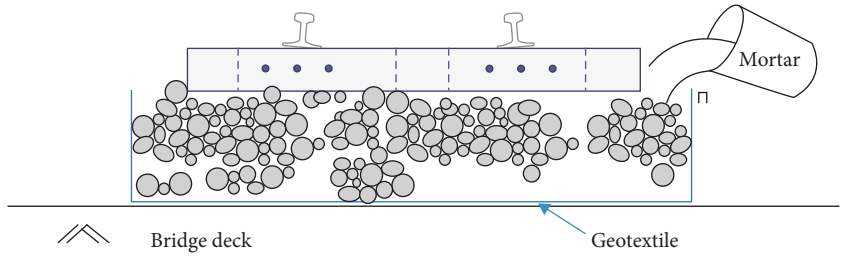

Figure 1: Concept of quick-hardening track.

infill materials for quick-hardening track were developed [3], and a quick-hardening track was installed in a 52 m length of a current railway line to verify the performance of the method [4]. The deformation characteristics of discontinuous sections of quick-hardening track were also examined as part of a full-scale test [5].

When a quick-hardening track is installed on bridges that occupy many sections of a high-speed railway line, the quick-hardening concrete must be firmly connected to, and structurally unified with, each bridge. To unify existing bridge decks with the quick-hardening track, the track must be secured with an anchor system capable of resisting the shear forces caused by the traction, braking, and driving operations of trains. Quick-hardening tracks on railway bridges are constructed with discontinuous segments (usually every 5 m) in order to compensate for the thermal expansion and contraction of the bridge. An anchor is installed at the center of each segment to minimize the thermal restraint force on the segment. Choi et al. [6] proposed a quick-hardening track system for bridges and analyzed the interaction between the system and a bridge. Although the anchor is the primary component that transfers the load to the bridge, the friction between a track slab with a wide surface area and the bridge deck must also be considered. Cho et al. [7] analyzed the behavior of the quick-hardening track on a bridge by considering the frictional characteristics between the track and the bridge.

In this study, two designs for the anchor system were proposed while considering the frictional characteristics between the track and bridge, and were experimentally verified to confirm the shear capacity. Trains running on tracks over a bridge generate loads in the transverse and longitudinal directions, respectively, both of which are considered in the anchor design. The longitudinal direction is the driving direction on a bridge, and the transverse direction is perpendicular to the bridge. Longitudinal loads are caused by the traction/braking actions of a train, vertically sloped track, and the expansion and contraction of continuous welded rail on a track. Transverse loads include the nosing force of a moving train, the centrifugal load generated by a train on a curved track, the wind load originating from lateral wind forces and applied to the side of a moving train, and the expansion-and-contraction loads caused by the expansion and contraction of a curved rail.

In this study, a friction test was conducted to identify the frictional coefficient between the quick-hardening track and bridge deck. With the design of the anchor system, loading tests were conducted in both the longitudinal and transverse directions to evaluate the corresponding shear load capacity. In reality, since such longitudinal and transverse loads are applied simultaneously, the anchor system connecting the quick-hardening track to a bridge is subjected to simultaneous longitudinal and transverse loads. In this regard, the structural capacity of the anchor systems, which were designed and separately tested for each direction, were also evaluated in terms of their biaxial shear capacity (i.e., both directions simultaneously) based on elliptical performance curves.

2. Anchor Design for Quick-Hardening Track on a Railway Bridge

2.1. Anchor System. To unify an existing bridge deck with a quick-hardening track during installation, it was decided to place the anchor brackets at the side of the track. Stud shear connectors were welded on the side of the anchor brackets to unify the brackets and the quick-hardening track. When construction of the track is complete, the brackets are unified with the bridge deck by postinstalling anchors through the bottom plate of the bracket into the bridge deck. Ultimately, the anchor system unifies the track with the bridge deck by way of the brackets, stud shear connectors, and postinstalled anchors.

The construction procedure for quick-hardening track on a railway bridge is illustrated in Figure 2. (a) The existing ballast track on the bridge is removed and anchor brackets are placed at the center of each quick-hardening track segment. (b) The surface of the bridge deck is covered with geotextile before a mold is constructed. The ballast that was removed from the existing track is then cleaned and poured into the mold. (c) Sleepers and rails are installed. (d) Additional ballast is laid. (e) Quick-hardening mortar is poured onto the ballast layer and quickly cured. (f) After curing is complete, anchor holes are drilled on the bridge deck through the holes of the anchor bracket, and then postinstalled anchors are installed.

2.2. Design Loads. When designing the anchor system, it is important to evaluate the design loads that can be applied to the anchor system in a single segment of quick-hardening track, and such design loads should consider both the longitudinal and transverse directions of the bridge. The maximum longitudinal loads are caused by a combination of

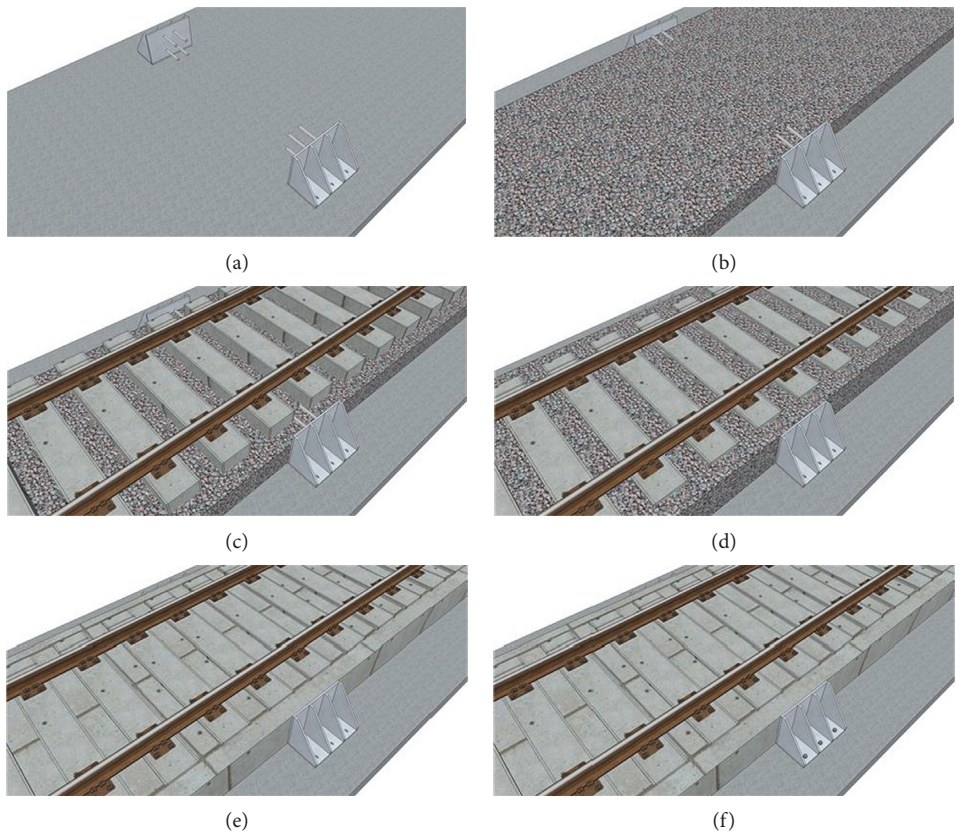

Figure 2: Concept of the anchor system for a quick-hardening track: (a) placing anchor brackets, (b) laying ballast, (c) installation of rails and sleepers, (d) laying additional ballast, (e) quick-hardening mortar injection and curing, and (f) installation of postinstalled anchors.

the traction/braking load, the track slope load, which depends on the slope of the track slab when the driving direction of track has a vertical slope, and the load generated by the thermal expansion and contraction of the continuous welded rail. In this study, 33.0 kN/m was applied as the traction load, which resulted in 165 kN of load for a single segment with a longitudinal length of 5 m. For the train load defined in KRL-2012 [8], which defines the Korean standard design load, an axle load of 220 kN and a distributed load of 80 kN/m were considered simultaneously. The track slope load was calculated to be 25.57 kN by reflecting the train load and self-weight of a single segment with the maximum slope of 2.5%. The expansion-and-contraction load of the continuous welded rail was calculated to be 50 kN for a single segment, which is obtained from the 10 kN/m specified in the Korea Design Standard [8]. As presented in Table 1, the ultimate longitudinal load (P_l) was calculated to be 342.02 kN with the load and combination factors specified in the design standard [9].

To calculate the maximum possible transverse load that can be applied to an anchor system, it is necessary to consider the nosing force of the train, the centrifugal force, which depends on the radius of curvature and the train velocity in the curved section, the wind load, and the thermal load of the rail. Based on the design standard, a nosing force of 25 kN/m was assumed to be applied throughout a longitudinal length of 4 m. Thus, the nosing force was calculated to be 100 kN. The centrifugal force was calculated for the axle and distributed loads of the train, respectively, by considering a high-speed railway bridge with a train velocity of 300 km/h, a bridge span length of 40 m, and a radius of curvature of 3500 m. A wind force of 1.50 kN/m^2 was considered to be horizontally applied to the side of the train (5×4.1 m). Finally, a rail load was applied in the transverse direction to account for the thermal expansion and contraction of the rail in a curved section. In this study, the rail load was calculated as the load applied to a single segment with a radius of curvature of 3500 m. According to the Korea Design Standard [8, 9], the total transverse load (P_t) was calculated to be 281.98 kN, as presented in Table 2.

A quick-hardening track segment is subjected to the maximum design load when the longitudinal and transverse design loads are applied simultaneously. Accordingly, the maximum possible design load on a quick-hardening track segment can be calculated by combining the longitudinal and transverse design loads (shown in the tables) as follows:

$$P_{\text{total}} = \sqrt{P_l^2 + P_t^2} = \sqrt{342.02^2 + 281.98^2} = 443.27 \text{ kN}. \quad (1)$$

When calculating the design loads applied to the anchor system, if the frictional resistance between the bridge deck and the quick-hardening segment is neglected, this may result in a conservative design in which the anchors are made to resist all the loads acting on the segment. However, as the segments contact the bridge deck over a large area, the

Table 1: Longitudinal design load (P_l) on a quick-hardening track segment.

Load type	Unfactored load (kN)	Load factor	Combination factor	Design load (kN)
Train traction load	165.00	1.50	1.00	247.50
Track slope load	25.57	1.35	1.00	34.52
CWR load	50.00	1.50	0.80	60.00
Total	—	—	—	342.02

Table 2: Transverse design load (P_t) on a quick-hardening track segment.

Load type	Unfactored load (kN)	Load factor	Combination factor	Design load (kN)
Nosing force	100.00	1.50	1.00	150
Centrifugal load (axle)	36.72	1.45	1.00	53.24
Centrifugal load (distributed)	33.38	1.45	1.00	48.40
Wind load	30.75	1.50	0.60	27.68
Rail load	2.21	1.50	0.80	2.66
Total	—	—	—	281.98

frictional resistance is considerable, which means that the actual load on the anchors of the quick-hardening segment can be significantly reduced [7]. This study considered the frictional resistance when evaluating the design load on the anchors of the quick-hardening segment in order to produce a more reasonable design. The actual design load on the anchors, which acknowledges the contribution of friction, can be calculated as follows:

$$P_{\text{anchor}} = P_{\text{total}} - \mu M \geq 0, \tag{2}$$

where μ is the friction coefficient between the track and the bridge deck and M is the weight of the track segment.

Figure 3 shows a plot of the design load on the anchor versus the friction coefficient. Based on the dimensions of the track segment, which are 5 m in the longitudinal direction of the bridge, 2.8 m wide, and 0.5 m thick, the corresponding weight of the segment is 174.37 kN. As shown in Figure 3, the design load on the anchor decreases as the friction coefficient increases. In particular, when the friction coefficient is 0.43 or above, the design load on the quick-hardening track is completely cancelled by the friction between the bridge deck and track, at which point the anchor system becomes unnecessary. The previous study [10] showed that when a low-frictional sliding layer consisting of a geotextile and PE sheet layer was installed between the concrete deck of the bridge and the track, the friction coefficient was about 0.3. As there was only the geotextile between the concrete deck and the quick-hardening track, the actual friction coefficient was expected to be higher than 0.3. In this study, the specimens were designed by conservatively assuming that the friction coefficient was 0.30, and the corresponding design load on the anchor system was calculated to be 136.36 kN.

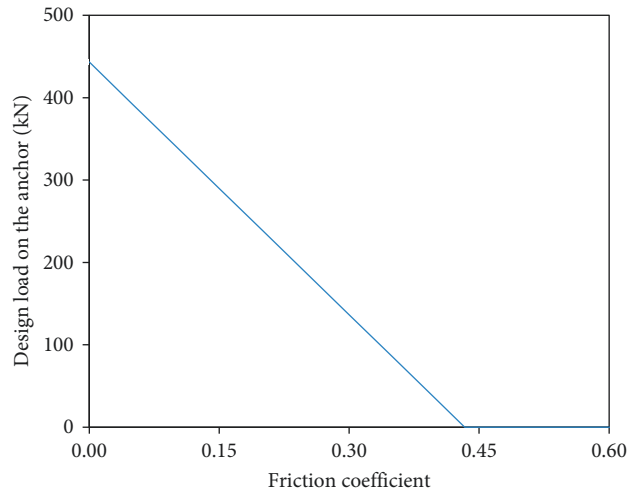

Figure 3: Design load on the anchor considering friction coefficient.

2.3. Materials. When designing the anchor system for the quick-hardening track segments on bridges, this study considered concrete with a nominal compressive strength of 24 MPa for the bridge deck. In addition, based on Lee and Pyo [4], quick-hardening concrete was assumed to have a 7-day compressive strength of 28 MPa. When considering the size of the quick-hardening track segments, the headed stud employed to unify the track and anchor brackets was assumed to have a tensile strength of 400 MPa or higher, a shank diameter of 19 mm, and a length (including the head) of 300 mm. The anchor brackets were fabricated from SM490 steel, which is widely used for structural members. The anchor bolts for the postinstalled anchor were HIT-Z M20 provided by HILTI. Figures 4 and 5 provide illustrations of the headed stud, postinstalled anchor bolt, and anchor filler.

2.4. Details of the Quick-Hardening Anchor Design. The stud shear connector joining the quick-hardening track and anchor bracket was specifically designed for this application. After the optimum number of studs was determined, the stud arrangement was finalized and the anchor bracket and postinstalled anchor were designed. The guidelines in AASHTO LRFD [11] and Eurocode-4 [12] were employed to determine the optimum number of headed studs to be used. Table 3 presents the design provisions for the shear strength

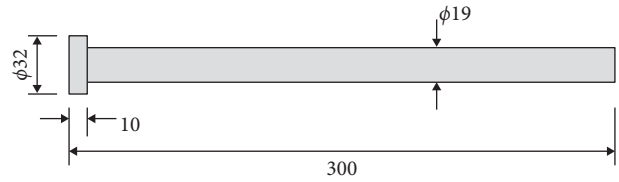

Figure 4: Details of the headed stud shear connector.

Figure 5: Postinstalled anchor bolts and filler.

of the headed stud in normal strength concrete as per the two referenced design codes. Based on the models, the design shear capacities for a single stud were calculated to be 96.4 kN and 68.4 kN from AASHTO LRFD [11] and Eurocode-4 [12], respectively. It was determined that two studs were sufficient to ensure the track system could support the anchor design load of 136.46 kN, which corresponds to a friction coefficient of 0.3.

The design strength of each stud and the required number of studs, which were calculated based on AASHTO LRFD [11] and Eurocode-4 [12], were determined based on the structural behavior of studs embedded in normal concrete; however, this behavior may be different from that of studs embedded in the quick-hardening track. In comparison to normal concrete in which the coarse aggregate has a maximum size of less than 25 mm, the maximum size of the coarse aggregate in quick-hardening concrete is larger than 40 mm, which negatively affects the structural behavior of the studs. In this regard, when considering the arrangement of studs on the anchor bracket side, it was determined to weld four studs to each anchor bracket side, which is double the number of studs required as per the design codes.

Postinstalled anchors were used to connect the bridge and anchor brackets. Two types of postinstalled anchors were identified that were suitable for use when the variability of the friction coefficient between the bridge deck and quick-hardening track was considered. As shown in Figure 6, for a friction coefficient of 0.3, Design A employed three postinstalled anchors set 220 mm apart in the longitudinal direction of the bridge. In contrast, Design B specified six postinstalled anchors set 260 mm apart in the longitudinal direction and 240 mm apart in the transverse direction to accommodate cases where the friction coefficient was relatively small.

The loading capacities of the postinstalled anchor systems were analyzed relative to the applied shear force along the anchor system and the concrete pryout around the bolts. This analysis was conducted with the HILTI PROFIS Anchor software package [13] using the design criteria provided in EOTA TR 029 [14]. As shown in Table 4, the loading capacity of each postinstalled anchor system exceeded the anchor design load in both designs.

Table 3: Design static strength of a stud shear connector.

Design code	Shear strength model
AASHTO LRFD [11]	$Q_r = \varnothing_{sc} Q_n = 0.5 \varnothing_{sc} A_{sc} \sqrt{f'_c E_c} \le \varnothing_{sc} F_u A_{sc}$ where Q_r and Q_n: design and nominal shear strength of a stud; $\varnothing_{sc}$: resistance factor which can be taken as 0.85; A_{sc}: cross-section area of a stud; f'_c: compressive strength of concrete; E_c: elastic modulus of concrete; F_u: ultimate tensile strength of a stud.
Eurocode-4 [12]	$P_{rd} = 0.29 \alpha d^2 \sqrt{f'_c E_c}/\gamma_v \le 0.85 F_u A_{sc}/\gamma_v$ where P_{rd}: design shear strength of a stud; α: depends upon the height-to-diameter ratio, h_{sc}/d is taken as $0.2(h_{sc}/d + 1)$ for $3 \le h_{sc}/d \le 4$ and 1 for $h_{sc}/d > 4$; γ_v: partial factor which can be taken as 1.25.

3. Experimental Program for the Anchors of Quick-Hardening Track

The loads that act on the anchors of a quick-hardening track segment on a bridge are inversely affected by the friction coefficient between the bridge deck and the quick-hardening concrete. In other words, as the friction coefficient increases, the actual load on the anchors decreases. Thus, evaluating the friction coefficient requires an analysis of the frictional behavior between the bridge deck and quick-hardening concrete.

When the maximum design load is actually applied to the anchor of a quick-hardening track segment on a bridge, the load is the combination of the longitudinal and transverse loads; however, this combination is difficult to represent in a structural test. Hence, in this study, the loads in the longitudinal and transverse directions of the bridge were evaluated separately. In other words, an experiment to evaluate the structural behavior was conducted for each direction, and the test results were used to evaluate the safety of the anchor versus the design loads placed on the anchor by the quick-hardening track.

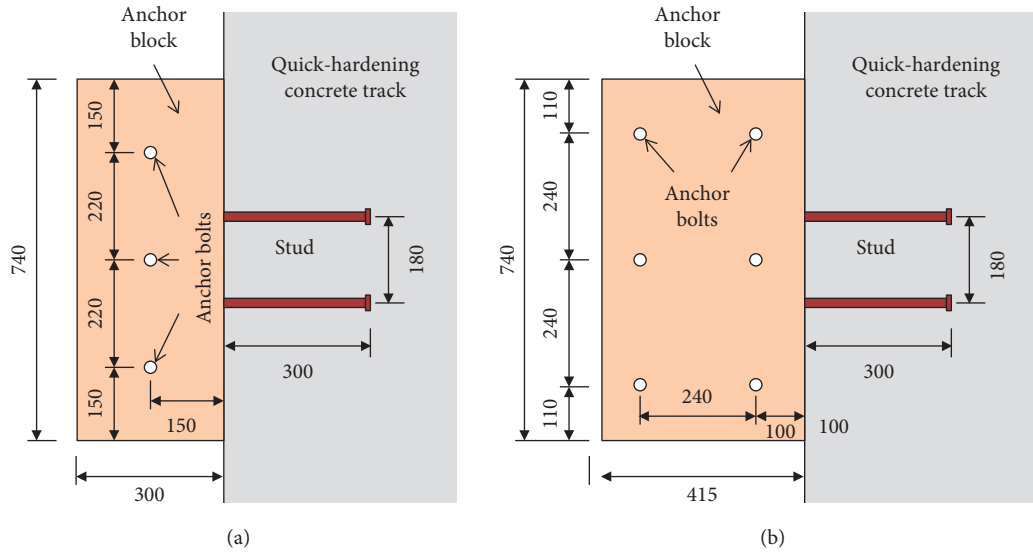

Figure 6: Overview of the anchor designs: (a) Design A and (b) Design B.

Table 4: Postinstalled anchor bolts design and the design load.

Design	No. of anchor bolts	Shear strength (kN)	Pryout strength (kN)	Design load (kN)	Note
Design A	3	175.20	136.78	136.36	OK
Design B	6	350.40	267.61	136.36	OK

Table 5: Test variables and the specimen names.

Specimen	Anchor bolts design	Track specimen dimension (m × m × m)	Loading direction	No. of specimens
AL	Design A	2.8 × 1.0 × 0.53	Longitudinal	1
AT	Design A	1.0 × 1.0 × 0.53	Transverse	1
BL	Design B	2.8 × 1.0 × 0.53	Longitudinal	2
BT	Design B	2.8 × 1.0 × 0.53	Transverse	2

With this in mind, three tests were conducted: the first was a friction test to analyze the frictional behavior between the bridge deck and the quick-hardening track, and the second and third were structural tests to identify the longitudinal and transverse structural behaviors, respectively. For purposes of efficiency, the specimen involving the Design A anchors were used for both the friction and transverse structural tests. After the friction test was completed, a postinstalled anchor was installed and then the transverse structural test was conducted. In addition, to ensure the reliability of the test results for larger loads, two specimens for each loading direction were fabricated as per Design B. Table 5 presents the test variables and main characteristics of the specimens involved in the longitudinal and transverse structural tests.

3.1. Details of Specimens. The frictional behavior of a quick-hardening track on a bridge can be experimentally measured by fabricating adequately sized specimens. Note that the transverse structural test should consider the situation wherein anchors are installed on only one side of the quick-hardening track when the load is applied to the opposite side. In the friction and structural tests for Specimen AT in which Design A was adopted, as shown in Figure 7(a), the quick-hardening track was chosen to be 1.0 × 1.0 m in size and anchors were installed on the opposite side to that where the loads were applied. As shown in the figure, the bridge deck was chosen to be 2.5 (longitudinal) × 2.0 m (transverse) in size. In the transverse structural test for Specimen BT in which Design B was adopted, a real-scale quick-hardening track specimen with a width of 2.8 m in the transverse direction of the bridge was fabricated.

When fabricating the specimens for the longitudinal structural test, anchors were installed on both sides of the quick-hardening track. In this case, real-scale quick-hardening track segments were fabricated with a transverse width of 2.8 m and a longitudinal length of 1.0 m, while considering the arrangement of the headed studs. In addition, a bridge deck was simulated by fabricating the deck of a specimen with a transverse width of 4.5 m. Figure 7(b) depicts Specimen AL, which employed the Design A anchor system. Specimen BL, which adopted the Design B anchor system, had the same details as Specimen AL, except that the anchor system was different.

3.2. Instrumentation. In the transverse structural behavioral test shown in Figure 7(a), linear variable displacement

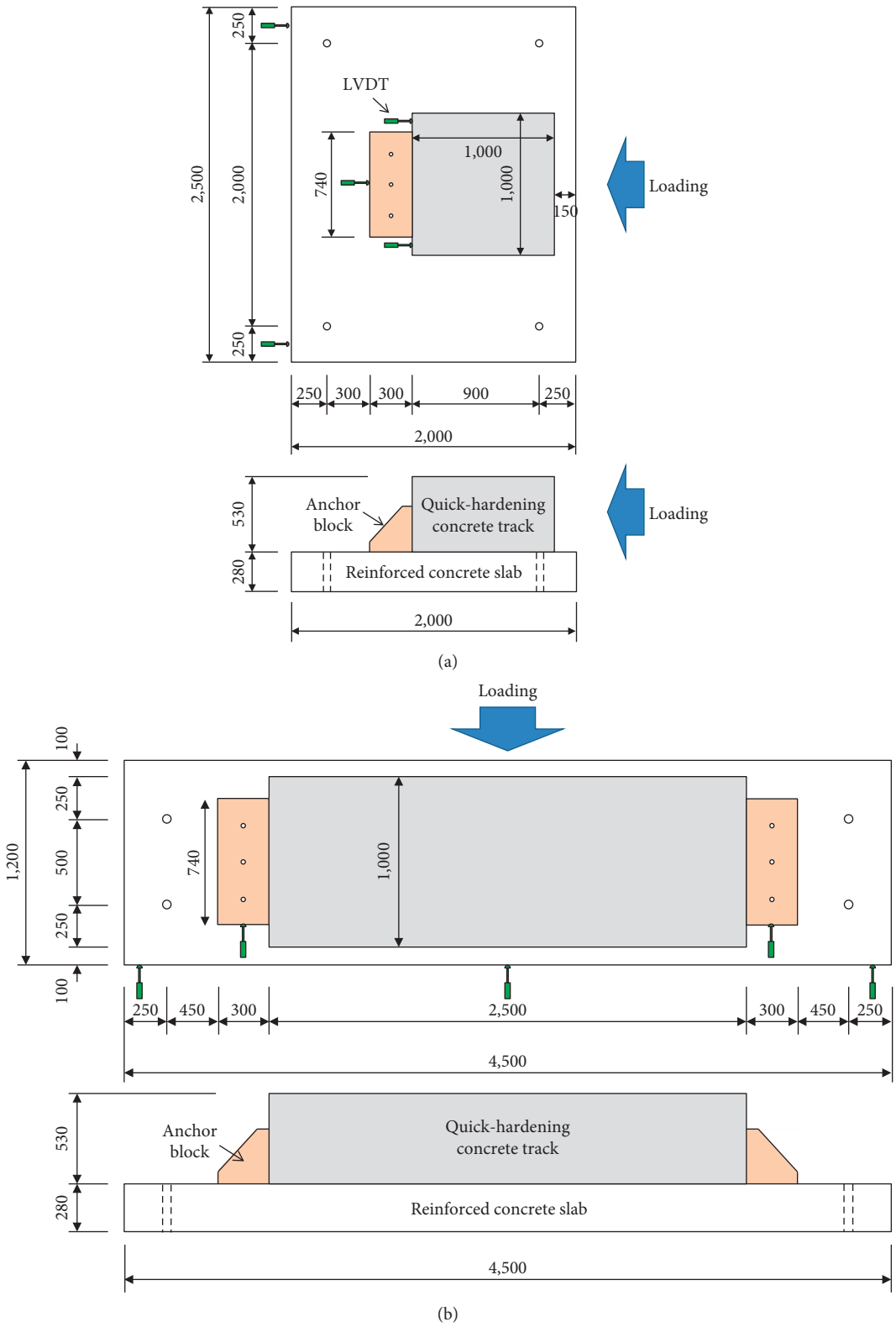

Figure 7: Details of the specimens and instrumentations: (a) Specimen AT and (b) Specimen AL.

transducers (LVDTs) were placed on each side of the quick-hardening track segment to measure the relative slip of the track from the deck. In addition, the slip of the anchor bracket was measured by placing one LVDT on each side of the anchor bracket. LDVTs were also installed on the deck to observe whether the deck exhibited unexpected slip during the test. In the longitudinal structural behavioral test shown in Figure 7(b), the relative slip of the quick-hardening track from the deck was measured through one LVDT at the center of the track. In addition, the slip of the anchor brackets and the deck was measured via LVDTs in the same way as in the transverse structural test.

3.3. Material Properties. When the decks were fabricated, three $\phi 100 \times 200$ mm cylindrical specimens were tested to determine their compressive strength. The concrete compressive strength of the decks was measured to be 28.2 MPa and 28.3 MPa for Designs A and B, respectively.

As the coarse aggregate of the quick-hardening concrete was around 40 mm in size, $\phi 150 \times 300$ mm cylindrical specimens were fabricated to measure the compressive strength when the quick-hardening track was first placed, and compression tests were conducted to assess the strength after various ages (days) had elapsed. The results of these tests are presented in Figure 8. As is clear from the figure, unlike normal concrete, the initial strength developed quite early. In the structural tests, the age of the quick-hardening concrete for the specimen conforming to Design A was 9–10 days, while that of the specimen conforming to Design B specimen was 28–30 days.

3.4. Test Procedure. A load was applied to the quick-hardening track at 1.0 mm/min when investigating the frictional and structural behaviors of the track. A wide steel plate or loading frame was placed between the hydraulic actuator and the quick-hardening track to ensure the load was uniformly distributed on the track. Since the first frictional test was expected to involve the influence of surface adhesion between the quick-hardening concrete and the deck, the frictional behavior test was conducted three times. In the longitudinal and transverse loading tests, a horizontal load was applied to the quick-hardening track until the maximum loading capacity was developed. Figure 9 shows the test setup used to evaluate the longitudinal and transverse behaviors for Specimens AL and AT, which conformed to Design A.

4. Test Results and Analysis for the Anchor of Quick-Hardening Track

4.1. Frictional Behavior. Figure 10 shows the frictional force-slip behavior measured in the friction test. As shown in this figure, the frictional resistance was measured to be around 8.5–9.0 kN in every round of the test. However, in the first friction test, the slip was measured to be 0.5 mm or higher when the static friction force had to be overcome and converted to kinetic friction, which

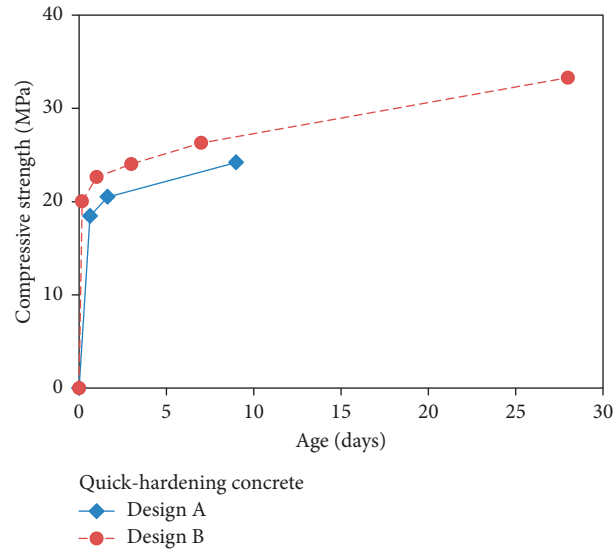

Figure 8: Compressive strength of quick-hardening concrete.

was larger than the slip of 0.1 mm measured in the second and third friction tests. This was thought to be a result of the surface adhesion between the quick-hardening concrete and the deck affecting the initial behavior in the first friction test. In reality, this initial adhesion will be quickly eliminated by the thermal expansion and contraction of the bridge and train operation after the track is placed. Therefore, the results of the second and third friction tests were used to evaluate the frictional behavior and friction coefficient in the quick-hardening track design.

The friction coefficient between the deck and the quick-hardening track can be calculated by dividing the measurement of the frictional force by the weight of the track (12.5 kN). From the test results, the average kinetic friction coefficients were calculated to be 0.684, 0.703, and 0.691 in the first, second, and third tests, respectively. Based on these, the friction coefficient was assumed to be 0.7 between the bridge deck and track when determining the load acting on the anchor system and evaluating the structural capacity of the design. However, it should be noted that water between the bridge deck and the quick-hardening track may be frozen in winter, which may decrease the friction coefficient to below the test results for dry geotextile. In this study, the objective is to determine the minimum allowable frictional coefficient while considering the shear capacity of the anchor system.

4.2. Longitudinal Structural Behavior. When the longitudinal structural behavior of the anchor systems was evaluated, the increase in the load caused cracks in the quick-hardening concrete around the anchor brackets. Then, as the damage of the concrete near the welded studs increased the slip, the load decreased for a short time before increasing again due to the support of the postinstalled anchor. After that, even if the slip increased, the load only increased slightly and the postinstalled anchor bolts were evidently damaged. Finally,

(a) (b)

Figure 9: Test setup: (a) Specimen AL and (b) Specimen AT.

an excessive slip occurred and caused the failure of the quick-hardening concrete near the studs welded to the anchor bracket, resulting in a drastic decrease in the load and forcing the termination of the test. Figure 11 shows the AL specimen after test, which is a representative failure behavior under longitudinal load.

Figure 12 illustrates the load-anchor bracket slip response measured during the longitudinal structural test. As shown in the figure, the longitudinal behavior can be classified into four phases. The first phase was dominated by the friction force between the deck and the quick-hardening concrete and occurred when the load was below the maximum frictional resistance. The second phase was dominated by the behavior of the studs welded to the anchor bracket and embedded in the quick-hardening concrete. The third phase involved an additional increase in the load due to the resistance of the postinstalled anchor bolts. The fourth phase exhibited plastic behavior. The first phase showed little slip in the quick-hardening concrete. Then, as the load increased, the studs provided resistance, which corresponds to the second phase. In particular, among the specimens incorporating Design B, Specimen BL-2 showed a temporary decrease in the load because of damage in the form of large cracks in the quick-hardening concrete near the studs at the end of the second phase. In the third and fourth phases, the resistance of the postinstalled anchor resulted in the maximum loading capacity.

In Figure 12, the maximum longitudinal loading capacity of the anchor systems was calculated by subtracting the friction force between the quick-hardening track and the deck from the maximum load measured during the test. If the weight of the quick-hardening track specimen is 34.8 kN and the friction coefficient is 0.7, the friction force becomes 24.4 kN. Therefore, the maximum longitudinal loading capacities of the anchor systems were calculated to be 433.5 kN for Design A and 766.0 kN for Design B.

Generally, when the shear resistance is calculated, which is commonly attributed to the dowel behavior of the rebar cast into the concrete member, the kinking effect is excluded and the behaviors up to the second phase are considered due to the bearing effect of the concrete supporting the dowel rebar [15–17]. In addition, the Korea Railway Network Authority specifies a limit of 2 mm on the maximum permissible horizontal displacement of a train-supporting structure [18]. If the above two considerations are considered for safety reasons when designing the anchor systems of the quick-hardening track, it seems reasonable to consider a 2 mm slip of the anchor bracket as part of the second phase behavior in the design. When the anchor bracket has a slip of 2 mm, the design loading capacities of the anchor systems were calculated to be 352.5 kN (Design A) or 519.3 kN (Design B). Table 6 briefly presents the procedure employed to calculate the longitudinal loading capacity of the anchor system from the test results.

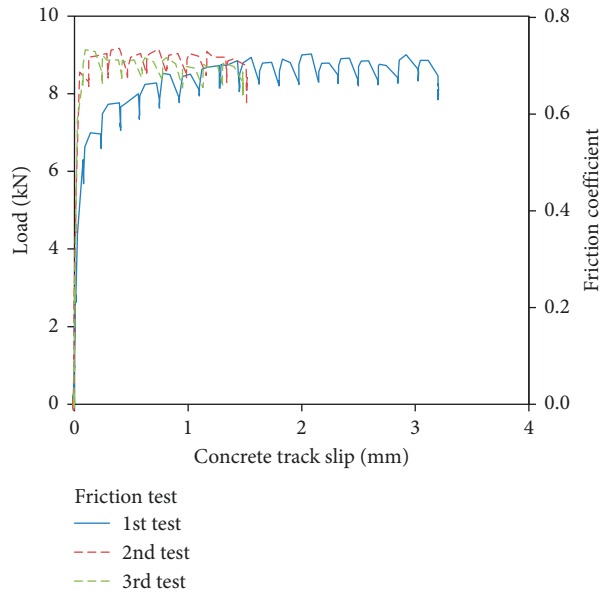

Figure 10: Load-slip response from the friction test.

4.3. Transverse Structural Behavior. Figure 13 shows the specimen after the transverse behavior test. As in the longitudinal behavior test, the postinstalled anchor bolts were damaged when the maximum loading capacity was developed. However, unlike the longitudinal behavior test, no damage was observed in the quick-hardening track.

(a) (b)

Figure 11: Failure of the specimen under the longitudinal load, Specimen AL: (a) damage on the anchor bolts and (b) crack pattern in concrete track.

Figure 14 shows the load-slip response of the quick-hardening concrete measured during the transverse structural test. As is clear from the figure, similar to the longitudinal behavior, the transverse behavior can also be classified into four phases. The first phase is dominated by the friction force between the deck and the quick-hardening concrete when the applied load is below the maximum frictional resistance. The second phase shows the complex behavior of the anchor bolts and the filler injected into the postinstalled anchor hole. The third phase involves an additional increase in the load due to the kinking effect of the postinstalled anchor bolt. Finally, the fourth phase exhibited plastic behavior. In the case of specimen BT-1, undesirable excessive rotation occurred due to the unintended eccentricity of the applied load, so the test was terminated earlier than that of the specimen BT-2.

In the same way as that of the longitudinal behavior, the maximum transverse loading and design loading capacities can be calculated by removing the friction force component between the deck and the quick-hardening track from the maximum load and the load corresponding to an anchor bracket slip of 2 mm, respectively. With these modifications, Design A was found to have a design loading capacity of 124.0 kN and a maximum loading capacity of 209.3 kN, while Design B had a design loading capacity of 188.5 kN and a maximum loading capacity of 393.1 kN. Table 6 briefly presents the procedure followed when calculating the transverse loading capacity of the anchor system from the test results.

4.4. Evaluation of the Biaxial Shear Capacity. As presented in Table 6, the calculated loading capacities of the anchor system indicate the individual loading capacities of the anchor system in each direction, that is, in the longitudinal and transverse directions. However, the actual design load acting on the anchor system of the quick-hardening track is the combination of the longitudinal and transverse loads. Therefore, when the maximum design load is applied in both directions, the actual maximum design load applied on the anchor system was found to be in a direction of about 39.5 degrees deflected from the transverse direction.

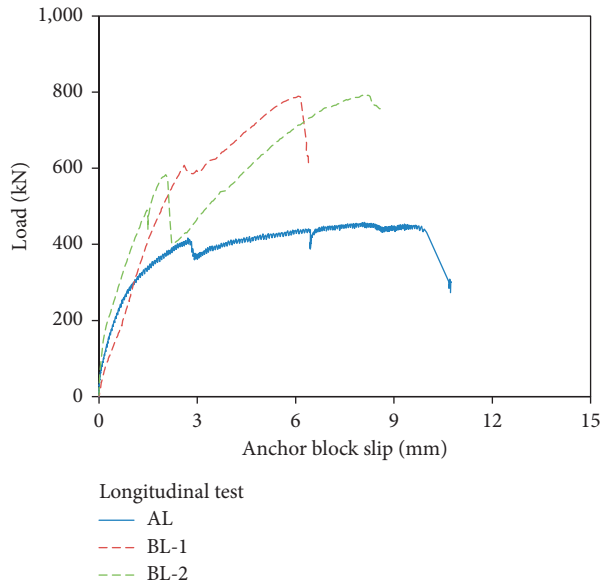

Figure 12: Longitudinal load-anchor block slip response.

To ensure the safety of the anchor under the given design load when calculating the loading capacity of the anchor system in each of the longitudinal and transverse directions, the loading capacity should also be calculated for the load in the actual direction. For this reason, in this paper, several yield criteria from the references were considered. As presented in Figure 15, three representative capacity curves were considered. When Rankine's yield criterion [19] is applied, the structural capacity of the anchor system may be overestimated. On the other hand, when the straight-line concept in maximum shearing stress theory [20] is adopted, the structural capacity of the anchor system may be underestimated. Therefore, this study employed an elliptical capacity curve [21] when evaluating the capacity of a reinforced concrete member under biaxial shear load. Here, based on the calculations of the longitudinal and transverse loading capacities of the anchor system, which themselves are based on the test results, the biaxial shear capacity curve of the anchor system can be expressed as follows:

Table 6: Shear loading capacity of the anchor systems from the experiments.

Specimen	Max. load (kN)	Load at a 2 mm slip (kN)	Frictional resistance (kN)	Ultimate loading capacity (kN)	Design loading capacity (kN)
AL	457.9	376.9	24.4	433.5	352.5
AT	218.0	132.7	8.7	209.3	124.0
BL	789.1	508.9	24.4	764.7	484.4
	791.6	578.6	24.4	767.2	554.1
BT	317.0	200.5	24.4	292.6	176.1
	518.0	225.3	24.4	493.6	200.9

(a) (b)

Figure 13: Damage on the anchor bolts under the transverse load: (a) Specimen AT and (b) Specimen BT.

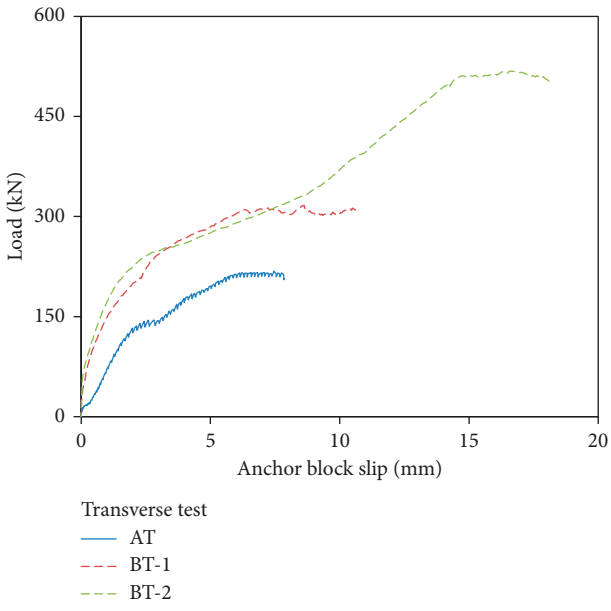

Figure 14: Transverse load-anchor block slip response.

$$\left(\frac{P_l}{P_{n,l}}\right)^2 + \left(\frac{P_t}{P_{n,t}}\right)^2 = 1, \tag{3}$$

where P_l and P_t are the longitudinal and transverse loads, respectively, acting on the anchor system, and $P_{n,l}$, $P_{n,t}$ are the loading capacities of the anchor system in the longitudinal and transverse directions, respectively.

Figure 16 compares the elliptical curve of the anchor system capacity and the design load while considering the various friction coefficients. If the design load acting on the anchor system is within the capacity curve, the anchor system is safe for the given design load. As shown in the figure, when the friction coefficient increases, the design load on the anchor system gradually decreases and thus the safety of the anchor system can be easily secured for the given loading conditions.

The allowable minimum friction coefficient between the bridge deck and the quick-hardening track to ensure the structural safety of the anchor system can be calculated by comparing the loads acting on the anchor system while considering the friction coefficient and the biaxial shear capacity curve. When the biaxial shear capacity curve is used, the allowable minimum friction coefficient in the event of a 2 mm slip of the anchor bracket was 0.258 in Design A and 0.168 in Design B. On the other hand, when the maximum loading capacity of the anchor was considered, the allowable minimum friction coefficient was calculated to be 0.156 in Design A, but the anchor structure was sufficient for safety irrespective of the friction coefficient in Design B. In this study, the friction coefficient between the deck and the quick-hardening concrete was measured to be about 0.7. If water in the gap between the bridge deck and the quick-hardening track is frozen during winter, the friction coefficient may decrease considerably, although it does not usually decrease below 0.3. Consequently, the proposed anchor systems were found to provide sufficient structural capacity versus the anticipated design loads acting on the anchor system that were considered in this study.

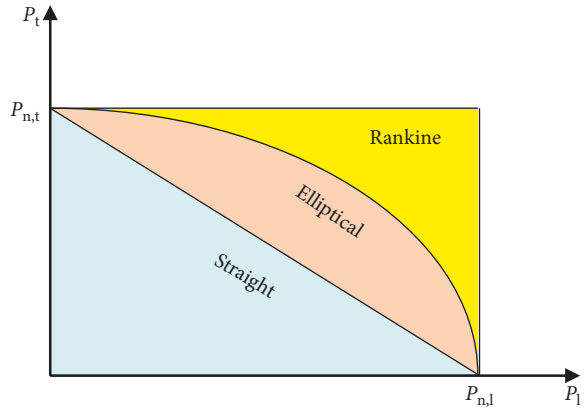

Figure 15: Failure criteria of biaxial shear for the anchor systems.

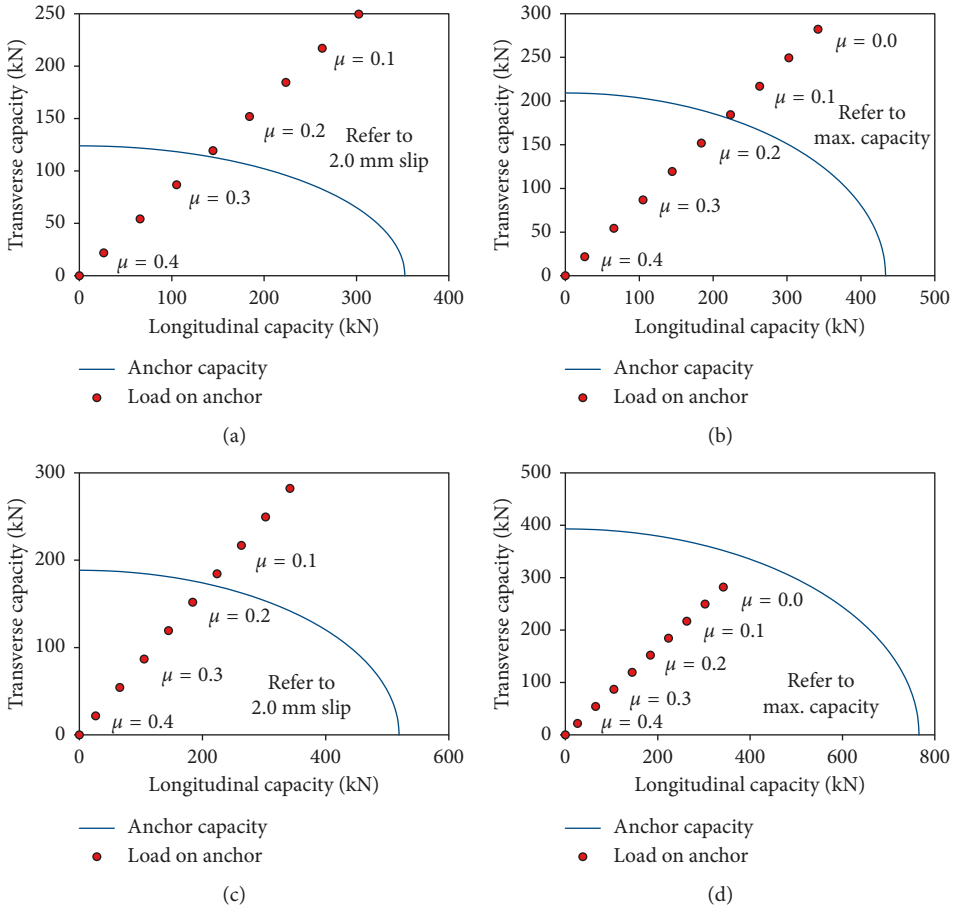

Figure 16: Investigation on structural safety considering friction coefficient and biaxial shear: (a) Design A with design loading capacity, (b) Design A with ultimate loading capacity, (c) Design B with design loading capacity, and (d) Design B with ultimate loading capacity.

5. Conclusions

In this study, an anchor system was proposed for the quick-hardening track on railway bridges while considering the friction forces between the bridge deck and track. Specimens were fabricated that were consistent with the proposed designs and were then used in friction tests and longitudinal and transverse structural tests. Based on the test results, the structural behavior of the proposed anchor system designs were analyzed and the allowable minimum friction coefficients were calculated to ensure structural safety. The primary conclusions of this study can be summarized as follows:

(1) Two designs were proposed for the anchor system that considered the variability of the friction coefficient, and both designs included postinstalled anchors and headed studs on the lateral anchor brackets attached on the side of the quick-hardening track. To accommodate the variation in friction, four-headed studs were installed on either side of the track and either three or six postinstalled anchor bolts were installed.

(2) In the friction test, the friction coefficient between the deck and the quick-hardening concrete was measured to be about 0.7. Since water can be frozen in the interface during winter, the corresponding decrease in the friction coefficient should be reflected in the design.

(3) The longitudinal and transverse loading capacities of the anchor systems were calculated by separating the friction force along the interface from the results of the longitudinal and transverse structural tests for the proposed anchor systems. Two types of loading capacity were considered: the maximum loading capacity corresponding to the maximum load and the design loading capacity corresponding to a 2 mm slip of the anchor bracket.

(4) When the anchor design load was evaluated using the elliptical biaxial shear capacity curve that was determined based on the longitudinal and transverse loading capacities of the anchor system, the proposed design displayed sufficient structural capacity to accommodate the given design loads.

(5) When the friction coefficient between the bridge deck and the quick-hardening track was 0.258 or above, the anchor system of Design A was sufficiently robust to ensure the structural safety of the track under the design loading capacity. Likewise, when the friction coefficient was 0.168 or above, Design B was able to ensure the structural safety of the track.

(6) The main results of this study will prove useful when designing anchor systems for quick-hardening track installed on railway bridges. In addition, this study will also be useful in the design and application of quick-hardening track on bridges.

Data Availability

All data have been presented in the manuscript, with tables and figures.

Conflicts of Interest

The authors declare that there is no conflict of interest regarding the publication of this paper.

Acknowledgments

This research was supported by a grant (18RTRP-B065581-06) from the Railroad Technology Research Program funded by the Ministry of Land, Infrastructure, and Transport of the Korean government.

References

[1] S. Y. Chang, I. W. Lee, and Y. S. Kang, "Track system technology for future advanced railway construction," *Journal of the Korean Society of Civil Engineers*, vol. 61, no. 9, pp. 41–51, 2013, in Korean.

[2] J. H. Hong, I. W. Lee, and W. Chung, "Behavior of the FHT on earthwork section considering thermal stress," *Journal of Korean Society of Hazard Mitigation*, vol. 15, no. 3, pp. 207–213, 2016, in Korean.

[3] I. W. Lee, S. Pyo, and Y.-H. Jung, "Development of quick-hardening infilling materials for composite railroad tracks to strengthen existing ballasted track," *Composites Part B*, vol. 92, pp. 37–45, 2016.

[4] I. W. Lee and S. Pyo, "Experimental investigation on the application of quick-hardening mortar for converting railway ballasted track to concrete track on operating line," *Construction and Building Materials*, vol. 133, pp. 154–162, 2017.

[5] I. Lee, Y.-T. Choi, S. Joh, and J. Um, "Deformation characteristics of discontinuous section of quick-hardening concrete tracks under full-scale test," *Proceedings of the Institution of Mechanical Engineers, Part F: Journal of Rail and Rapid Transit*, vol. 231, no. 3, pp. 255–268, 2017.

[6] W. Choi, H. Lee, I. Lee, S. Y. Jang, and W. Chung, "Behavior analysis of fast hardening track on the bridge," *Journal of Korean Society of Hazard Mitigation*, vol. 17, no. 1, pp. 203–208, 2017, in Korean.

[7] S.-H. Cho, I.-W. Lee, W.-S. Chung, H.-Y. Lee, and K.-C. Lee, "Track-structure interaction analysis of fast hardening track on railway bridge considering effect of anchor and friction," *Journal of computational structural engineering institute of Korea*, vol. 31, no. 1, in Korean, 2018.

[8] Korea Design Standard, KDS 24 12 20:2016, *Bridge Design Load (General Design Method)*, Korea Construction Standards Center, Goyang, Gyeonggi-do, Republic of Korea, 2016.

[9] Korea Design Standard, KDS 24 12 10:2016, *Bridge Design Load Combination (General Design Method)*, Korea Construction Standards Center, Goyang, Gyeonggi-do, Republic of Korea, 2016.

[10] T.-G. Kim, D.-K. Jung, and K.-C. Lee, "Experimental study of low-frictional behavior for sliding slab track," *Journal of the Korean Society for Railways*, vol. 20, no. 2, pp. 241–247, 2017, in Korean.

[11] AASHTO, *AASHTO LRFD Bridge Design Specifications*, American Association of State Highway and Transportation Officials, Washington, DC, USA, 2012.

[12] CEN, 1994-2 Eurocode 4, *Design of Composite Steel and Concrete Structures. Part 2, General Rules and Rules for Bridges*, 2005.

[13] Hilti PROFIS Anchor Software, https://www.hilti.com/2097332.

[14] EOTA TR 029, *Design of Bonded Anchors*, p. 36, European Organisation for Technical Approvals, Brussels, Belgium, 2010.

[15] N. Randl, "Load bearing behaviour of cast-in shear dowels," Vol. 102, pp. 31 -37, Beton- und Stahlbetonbau, 2007.

[16] Comité Euro-International du Béton, *Fib Model Code for Concrete Structures 2010*, p. 402, Ernst & Sohn, Berlin, Germany, 2013.

[17] S.-C. Lee, S. Park, J. Lee, and K.-C. Lee, "Dowel behavior of rebars in small concrete block for sliding slab track on railway bridges," *Advances in Materials Science and Engineering*, vol. 2018, pp. 1–15, 2018.

[18] *Korea Rail Network Authority, KR C-08050 Deflection*, KR Network, Dajeon, Republic of Korea, 2012.

[19] W. Rankine, "On the stability of loose earth," Philosophical Transactions of the Royal Society of London, vol. 147, 1857.
[20] H. Tresca, *Mémoire sur l'écoulement des corps solides soumis à de fortes pressions*, Gauthier-Villars, Vol. 59, p. 754, Gauthier-Villars, Paris, 1864.
[21] C. Hansapinyo, K. Maekawa, and T. Chaisomphob, "Behavior of reinforced concrete beams subjected to biaxial shear," *Journal of Materials, Concrete Structures and Pavements*, vol. 725, no. 58, pp. 321–331, 2003.

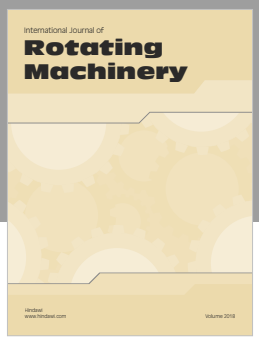

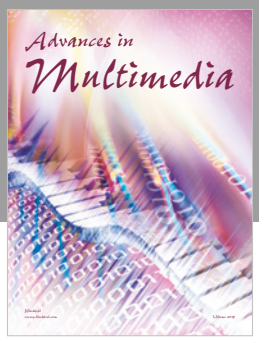

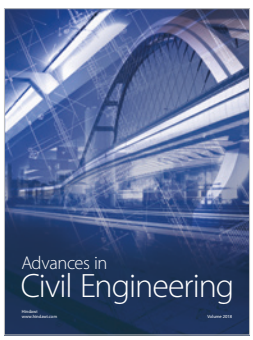

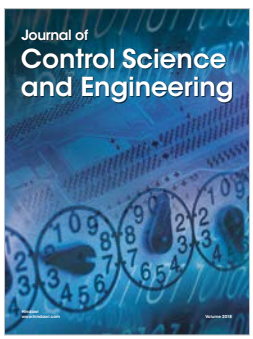

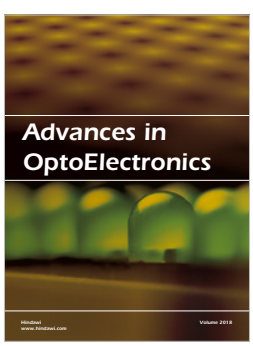

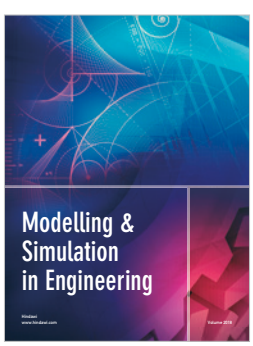

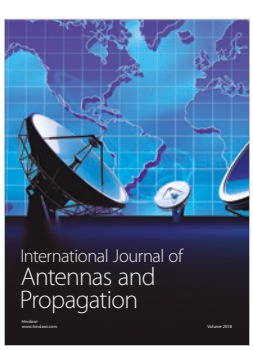

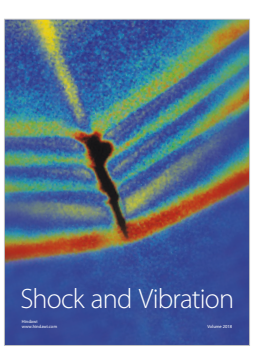

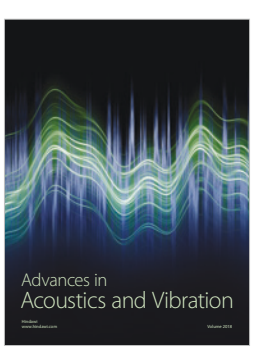

Hindawi

Submit your manuscripts at
www.hindawi.com